Mass media interventions and social reinforcements drive rumor propagation

Yafang Dong [1,2,3] Liang'an Huo [2,4,*] Matjaž Perc [5,6,7,8,†] and Stefano Boccaletti [3,9,10,11,‡]

[1] *College of Shanghai Lausanne Hospitality Management, Shanghai Business School, Shanghai 200233, China*
[2] *Business School, University of Shanghai for Science and Technology, Shanghai 200093, China*
[3] *Institute of Complex Systems, CNR, Via Madonna del Piano 10, Sesto Fiorentino, Florence, 50019 Firenze, Italy*
[4] *School of Intelligent Emergency Management, University of Shanghai for Science and Technology, Shanghai 200093, China*
[5] *Faculty of Natural Sciences and Mathematics, University of Maribor, Koroška cesta 160, 2000 Maribor, Slovenia*
[6] *Community Healthcare Center Drive Adolf Drolc Maribor, Ulica talcev 9, 2000 Maribor, Slovenia*
[7] *Department of Physics, Kyung Hee University, 26 Kyungheedae-ro, Seoul 02447, Republic of Korea*
[8] *University College, Korea University, 145 Anam-ro, Seoul 02841, Republic of Korea*
[9] *Sino-Europe Complexity Science Center, School of Mathematics, North University of China, 3 Xueyuan Road, Taiyuan, Shanxi 030051, China*
[10] *Research Institute of Interdisciplinary Intelligent Science, Ningbo University of Technology, Ningbo, Zhejiang 315104, China*
[11] *International Research Center of Complexity Sciences, Hangzhou International Innovation Institute, Beihang University, Hangzhou 311115, China*

(Received 20 April 2026; revised 28 July 2026; accepted 25 September 2026; published 2 November 2026)

Rumors now spread faster and wider than ever, driven by diverse communication channels. To capture this complexity, we develop a multilayer coupled model of rumor propagation that integrates individual behavioral differences, mass media influence, social reinforcement, and the interplay of cooperative and competitive dynamics across channels. Using mean-field theory, we analyze the system's dynamics and derive the critical threshold through the next-generation matrix method. Numerical simulations show that traditional mass media interventions are more effective in limiting single-channel spreaders, while new media interventions have stronger effects on dual-channel spreaders. However, when traditional mass media pressure is already high, intensifying new media interventions may fail to suppress offline spreaders and can instead raise costs or even cause negative outcomes. We also find that dual-channel spreaders are more responsive to changes in online rumor prevalence and play a stronger role in overall rumor dynamics than single-channel spreaders. Finally, validation with a Twitter dataset confirms the model's predictive power for offline rumor spread.

DOI: 10.1103/vxkg-41kp

I. INTRODUCTION

Rumors, as a special form of information propagation, are often characterized by uncertainty and negative consequences. Their spread can trigger panic, erode trust, and even cause social unrest, thereby threatening public stability and order [1–3]. During public health emergencies, rumors create information asymmetry that misleads the public and influences decision-making. The COVID-19 pandemic highlighted how rapidly health misinformation can spread through online platforms and continue to shape public behavior despite subsequent official corrections [4]. With the rise of social media, such rumors now spread faster and reach wider audiences than ever before. Understanding the mechanisms of rumor propagation is therefore crucial for developing strategies to manage information and maintain social stability.

Because rumor spread resembles the transmission of epidemics, researchers have frequently drawn on epidemiological theories and models. Daley and Kendall introduced the classical DK model [5], followed by Maki and Thompson's MT model, which refined the treatment of spreader behavior [6]. These early models laid the foundation for a mathematical understanding of rumor dynamics. Later, the role of network topology became central, as the spread of information depends not only on rumor characteristics but also on the structure of relationships among individuals. Zanette pioneered the study of rumor propagation on complex networks, demonstrating its dynamics on small-world topologies [7,8]. Since then, many studies have examined how different network structures shape the spread of rumors [9–12].

Beyond network topology, a variety of other factors influence rumor propagation. These include time delays [13–15], the attractiveness or ambiguity of rumor content [16], emotional states of individuals [17,18], environmental noise [19–21], and media coverage [22,23]. Among these, the mass media have received particular attention. For example, Guo et al. showed that media refutation combined with individual contrarian behavior can effectively suppress rumors [24], while Huo et al. analyzed stochastic models including media coverage and noise, demonstrating that greater coverage reduces the extent of spread [25]. However,

*Contact author: huohuolin@yeah.net
†Contact author: matjaz.perc@gmail.com
‡Contact author: stefano.boccaletti@gmail.com

 ©2026 American Physical Society

most existing research treats mass media narrowly, focusing on traditional outlets such as television and radio. In contrast, new forms of mass media—especially social media platforms and personalized news feeds—operate under very different dynamics. Their emergence highlights the heterogeneity of media environments, as traditional and new media exert distinct influences on information dissemination depending on their mechanisms and audiences.

Another key factor shaping rumor dynamics is social reinforcement, which captures how repeated exposures influence individual behavior. Reinforcement creates a paradox. In theory, positive feedback between exposure and sharing probability should generate explosive spread, but in practice, such cascades are rare. Empirical studies suggest that repeated encounters with the same message often reduce the likelihood of resharing, a phenomenon sometimes described as "information fatigue" [26–29]. We refer to this counterintuitive effect as negative social reinforcement. Understanding its role is essential for explaining why rumors sometimes fail to achieve widespread diffusion despite high visibility.

Communication theory also emphasizes the importance of the communication channel, alongside the source, message, and receiver [30]. Historically, rumors spread mainly through offline word-of-mouth, which has often been modeled using single-layer networks. The rapid growth of the internet, however, has introduced online platforms as a dominant channel. To analyze interactions across both online and offline spaces, multilayer network theory provides a natural framework. Such networks consist of multiple interconnected layers, each with distinct structural and dynamical properties [31,32]. Recent research has examined multilayer dynamics across a variety of domains, including the coevolution of epidemic spread and awareness [33,34], diffusion of multiple types of knowledge [35], creative diffusion [36], and other processes [37]. Yet, despite these advances, the complex interactions among communication channels in rumor propagation remain underexplored.

These interactions involve both cooperation and competition. On the cooperative side, information from one channel can strengthen an individual's ability to disseminate it through another—for instance, online exposure may enhance offline discussion. On the competitive side, reliance on one channel may reduce attention and resources allocated to another. Mass media interventions also illustrate this duality. Media refutations can suppress rumor spread across both online and offline networks, but individuals who simultaneously attend to multiple channels may allocate less cognitive attention to mass media, weakening their effectiveness. These interactions suggest that rumor propagation is not simply the superposition of multiple communication channels. Instead, the collective spreading dynamics emerge from the interplay among heterogeneous communication behaviors, repeated social reinforcement, and media intervention. Understanding how these mechanisms jointly reshape the macroscopic spreading dynamics, particularly the shift between cooperative and competitive inter-layer interactions, constitutes the central scientific question addressed in this work.

Despite extensive prior work, important research gaps remain. First, many studies focus on either single-layer networks or simplified multilayer structures, leaving the rich interplay among online, offline, and mass media channels insufficiently understood. In particular, the role of limited cognitive resources in constraining cross-channel attention has received little attention. Second, most research treats mass media as a uniform entity, neglecting the clear distinctions between traditional media such as television and radio and newer forms such as social media and news apps. These platforms differ in their audiences, dissemination mechanisms, and interactions with other channels, suggesting the need for a more nuanced treatment. Third, individual heterogeneity in channel use is often overlooked. In reality, some individuals share information primarily online, others primarily offline, and some across both domains. This diversity gives rise to distinct communication behaviors, allowing us to investigate how single-channel and dual-channel spreaders contribute differently to rumor propagation across multiple communication channels. Such heterogeneous communication behaviors provide the microscopic basis for the emergence of cooperative and competitive interactions across different communication channels.

Collectively, these limitations prevent existing models from systematically investigating how multiple communication mechanisms interact to shape rumor spreading dynamics across heterogeneous communication channels. To address these gaps, we develop a multilayer rumor propagation framework that integrates heterogeneous communication behaviors, social reinforcement, and heterogeneous mass media. The purpose of introducing these mechanisms is not simply to construct a more realistic model, but to investigate how their interplay reshapes rumor spreading across multiple communication channels. Specifically, the proposed framework enables us to (i) distinguish the dynamical roles of single-channel and dual-channel spreaders, (ii) quantify the different influences of traditional and new mass media, and (iii) reveal how interactions between online and offline communication evolve from cooperative to competitive regimes. The proposed framework provides mechanistic insights into rumor propagation across heterogeneous communication channels and is further validated using Twitter data.

The remainder of this paper is organized as follows. Section II introduces the multilayer coupled model, formulated through mean-field theory. Section III presents the results, including the theoretical analysis, the numerical simulations, and the model verification. Section IV concludes with a discussion of the main findings.

II. MODEL

A. Three-layer coupled network construction

Data from advertising planning tools of leading social media platforms reveals that by the end of 2025, there were approximately 1.07 billion social media users aged 18 and above in China, accounting for 93.8 percent of the adult population. Moreover, 98.6 percent of China's total internet users, regardless of age, were active on at least one social media platform in October 2025 [38]. While the Internet has significantly enhanced convenience in daily life, it has also

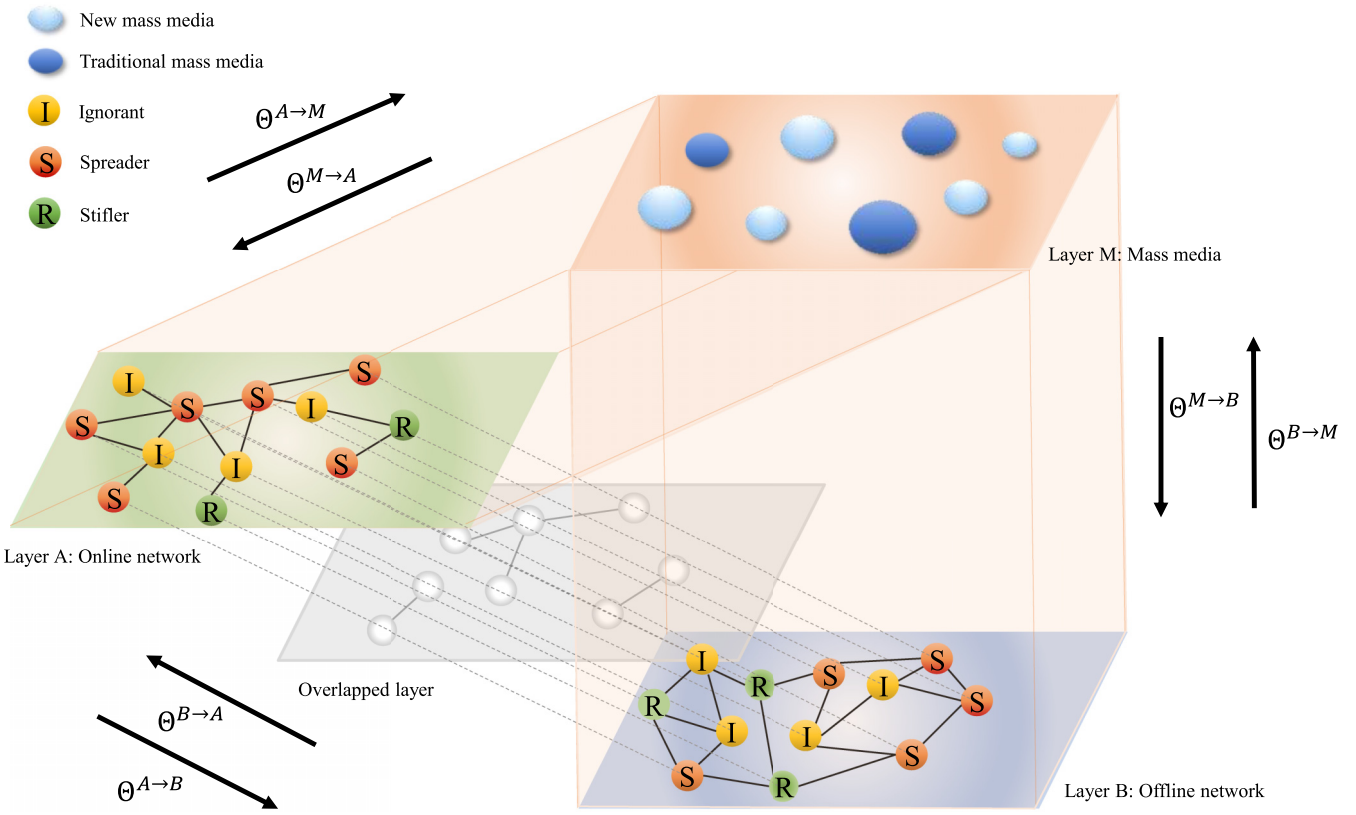


FIG. 1. Schematic illustration of the three-layer coupled rumor propagation model. The system consists of a mass media layer M, an online social network layer A, and an offline physical contact layer B. Layer M represents heterogeneous mass media sources, including new mass media (light blue spheres) such as online news platforms and traditional mass media (dark blue spheres) such as television, newspapers, and radio, depicted as ellipses of varying sizes. Layer A consists of virtual accounts and their online connections, modeled as a scale-free network $A(V_A, E_A)$. Layer B represents real-world individuals and their physical contacts, modeled as a homogeneous mixed network $B(V_B, E_B)$. Each node in layer A is mapped to a corresponding node in layer B, capturing the interplay between online and offline behaviors. Rumor information can spread via both online and offline channels, with shared nodes and edges forming an overlapping region between A and B. Node colors represent individual states: ignorants (I, yellow), spreaders (S, red), and stiflers (R, green). Inter-layer interactions are characterized by the effective coefficients $\Theta^{X\to Y}$, where the superscript indicates the direction of influence from layer X to layer Y. The detailed mathematical definitions are given in Eqs. (17)–(22).

provided a fertile ground for the rapid and widespread dissemination of rumors.

Through social media registration, individuals can quickly establish extensive social networks, sharing information globally without the constraints of geography. Online social networks differ structurally and functionally from offline networks, yet the same individual often connects both, allowing information to flow seamlessly between the two. This integration of online and offline channels fosters synergistic effects, enabling the accelerated spread of rumors and potentially leading to severe negative consequences.

To curb the spread of rumors, mass media frequently intervene. The effectiveness of such interventions depends on mass media heterogeneity, which encompasses variations in the types, characteristics, and functions of mass media channels. These variations include differences in format (e.g., television, radio, online platforms), audience scope (e.g., national vs local, general vs specialized), and content style (e.g., news, entertainment, educational). In this paper, mass media refers to both traditional mass media, such as television, radio, newspapers, and magazines, and new mass media, including public accounts on social media platforms and aggregators like Google News. These platforms are typically managed by professional media organizations or guided by editorial policies, ensuring the propagation of accurate information to counteract rumors. This categorization underscores the distinctive roles and impacts of traditional and modern media in mitigating rumor propagation dynamics.

A three-layer coupled rumor propagation model is developed to investigate how interactions among the online network layer, the offline network layer, and the mass media layer influence the dynamic process of rumor propagation, as schematically illustrated in Fig. 1.

Specifically, individuals receive information through three primary channels: mass media, online social media, and offline physical interactions. Mass media primarily propagates positive information, which plays a crucial role in suppressing the spread of rumors. To represent these three propagation channels, a coupled hierarchical network is employed, leading to the construction of a three-layer coupled network model. Notably, individuals may propagate rumors through both online and offline channels, creating an overlapping layer

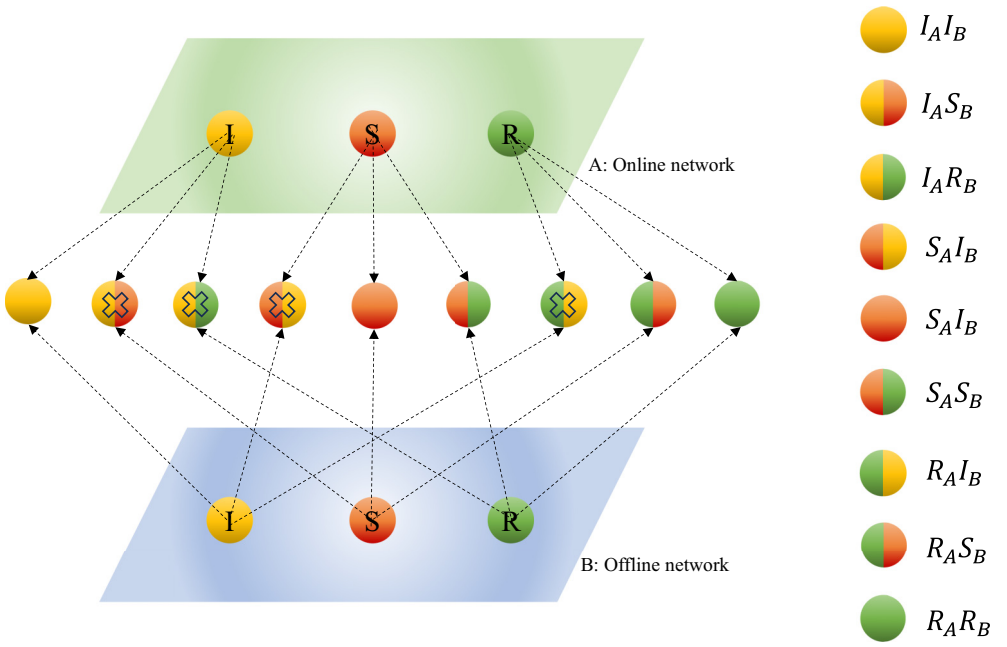


FIG. 2. Node state classification in the online layer A and offline layer B. Individuals are categorized into three basic states: ignorant (I), spreader (S), and stifler (R), in each layer. Different sharing behaviors across channels allow an individual to occupy different states in A and B, leading to nine possible state combinations I_AI_B, I_AS_B, I_AR_B, S_AI_B, S_AS_B, S_AR_B, R_AI_B, R_AS_B and R_AR_B. Since an individual cannot be both informed and uninformed simultaneously, only five combinations are effective: I_AI_B, S_AR_B, R_AS_B, S_AS_B and R_AR_B. Here, S_AR_B denotes an online single-channel spreader, R_AS_B denotes an offline single-channel spreader, and S_AS_B denotes a dual-channel spreader.

between layers A and B. This overlapping layer, consisting of shared nodes and edges, highlights the interconnected nature of rumor propagation across different communication channels.

Building on this structure, we proceed to describe the modeling assumptions and define the relevant parameters. The online social network is modeled as a scale-free network, reflecting the highly heterogeneous nature of individual interactions, where the number of neighbors an individual contacts per unit time, denoted by k, varies significantly across nodes. Conversely, the offline network is assumed to be a homogeneous mixed network, in which all individuals interact with a roughly equal number of neighbors per unit time, denoted by a constant C. The total population size is represented by N.

To represent external intervention, we consider two types of mass media: new mass media and traditional mass media. The former primarily affects the online network layer and exerts influence at a constant intensity m_1, i.e., the number of times the new mass media propagates official information to the public within the online network layer. while the latter influences the offline layer with intensity m_2, i.e., the number of times the traditional mass media propagates official information to the public within the offline network layer. Let $N_{(m_1,m_2,k,C)}$ denote the number of individuals characterized by parameters (m_1, m_2, k, C). The probability that a randomly selected node in the online layer has degree k is given by $p(k) = \frac{N(m_1,m_2,k,C)}{N}$, and the average degree of the online network is $\langle k\rangle = \sum_{k=0}^{n} kp(k)$. During unit time at moment t, the probability that an ignorant individual of degree k randomly contacts a neighbor of degree l is denoted by $p(l|k)$, and the probability that a node of degree l is in the state of spreader S is $\frac{S(m_1,m_2,l,C)}{N(m_1,m_2,l,C)}$. Therefore, the probability that an ignorant individual I of degree k contacts a spreader during online communication in unit time is $\sum_{l=1}^{n} p(l|k)\frac{S(m_1,m_2,l,C)}{N(m_1,m_2,l,C)}$.

B. Rumor propagation mechanism

Building upon the network structure and interaction probabilities described above, we next classify the possible joint states of individuals within the coupled online-offline layers and outline the corresponding rumor propagation rules. The coupled online-offline network allows individuals to occupy different states in each layer. We classify these joint states into five effective combinations, as illustrated in Fig. 2.

In a rumor propagation system, rumors can be propagated within layers or between layers through individual interactions. The propagation rules obey the following assumptions.

1. Intralayer propagation rules in the online social network layer A

The intralayer propagation probability of the dual-channel spreader S_AS_B is β_A, the intralayer immunization probability of the dual-channel stifler R_AR_B is α_A, and it is assumed that the willingness to propagate of the dual-channel spreader S_AS_B will be higher than that of the single-channel spreader S_AR_B, and the immunization probability of the dual-channel stifler R_AR_B will be higher than that of the single-channel spreader R_AS_B. These relationships are subsequently expressed in terms of a willingness reduction factor ω. Then we have $\beta_C = \omega\beta_A$, $\alpha_C = \omega\alpha_A$.

The specific propagation rules are as follows:

$$I_A I_B + S_A R_B \xrightarrow{\beta_C} S_A R_B + S_A R_B, \tag{1}$$

$$I_A I_B + S_A S_B \xrightarrow{\beta_A} S_A R_B + S_A S_B, \tag{2}$$

$$R_A S_B + S_A R_B \xrightarrow{\beta_C} S_A S_B + S_A R_B, \tag{3}$$

$$R_A S_B + S_A S_B \xrightarrow{\beta_A} S_A S_B + S_A S_B, \tag{4}$$

$$S_A R_B + R_A S_B \xrightarrow{\alpha_C} R_A R_B + R_A S_B, \tag{5}$$

$$S_A R_B + R_A R_B \xrightarrow{\alpha_A} R_A R_B + R_A R_B, \tag{6}$$

$$S_A S_B + R_A S_B \xrightarrow{\alpha_C} R_A S_B + R_A S_B, \tag{7}$$

$$S_A S_B + R_A R_B \xrightarrow{\alpha_A} R_A S_B + R_A R_B. \tag{8}$$

2. Intralayer propagation rule in the offline contact network layer B

The intralayer propagation probability of a dual-channel spreader $S_A R_B$ is β_B, and the intralayer immunization probability of a dual-channel stifler $R_A R_B$ is α_B. Similarly, it is assumed that the willingness to propagate of a dual-channel spreader $S_A S_B$ will be higher than that of a single-channel spreader $R_A S_B$, and the immunization probability of a dual-channel stifler $R_A R_B$ will be higher than that of a single-channel spreader $S_A R_B$. Similarly, these relationships are subsequently expressed in terms of a willingness reduction factor ω. Then we have $\beta_D = \omega\beta_B$, $\alpha_D = \omega\alpha_B$,

$$I_A I_B + R_A S_B \xrightarrow{\beta_D} R_A S_B + R_A S_B, \tag{9}$$

$$I_A I_B + S_A S_B \xrightarrow{\beta_B} R_A S_B + S_A S_B, \tag{10}$$

$$S_A R_B + R_A S_B \xrightarrow{\beta_D} S_A S_B + R_A S_B, \tag{11}$$

$$S_A R_B + S_A S_B \xrightarrow{\beta_B} S_A S_B + S_A S_B, \tag{12}$$

$$R_A S_B + S_A R_B \xrightarrow{\alpha_D} R_A R_B + S_A R_B, \tag{13}$$

$$R_A S_B + R_A R_B \xrightarrow{\alpha_B} R_A R_B + R_A R_B, \tag{14}$$

$$S_A S_B + S_A R_B \xrightarrow{\alpha_D} S_A R_B + S_A R_B, \tag{15}$$

$$S_A S_B + R_A R_B \xrightarrow{\alpha_B} S_A R_B + R_A R_B. \tag{16}$$

For the subsequent analysis, $I_A I_B$ is denoted by I, $S_A R_B$ by S_1, $R_A S_B$ by S_2, $S_A S_B$ by S_3, and $R_A R_B$ by R, where the corresponding densities are denoted by i, s_1, s_2, s_3, and r, respectively.

3. Interaction rules among the three layers

To characterize the strength of inter-layer interactions, we introduce $\Theta^{X\to Y}$ to denote the effective influence exerted by layer X on layer Y, where $X, Y \in \{A, B, M\}$. Depending on the interaction considered, Θ represents either a cooperative interaction strength or a media-induced suppression coefficient.

First, there is a cooperative and competitive coexistence between the online social network layer A and the offline physical contact layer B. Specifically, in the early stage of rumor propagation, individuals' propagation in one layer will promote their propagation in the other layer, but according to the self-exhaustion theory [39], individuals' energy is limited, so in the later stage, individuals' propagation in one layer will inhibit their propagation in the other layer, i.e., there are

$$\Theta^{A\to B} = \frac{\theta\langle k\rangle}{\langle k\rangle + |C_0 - \langle k\rangle|}, \tag{17}$$

$$\Theta^{B\to A} = \frac{\theta C}{C + |C_0 - C|}, \tag{18}$$

where θ denotes the base interaction rate between online and offline channels, $\langle k\rangle$ denotes the average number of times an individual communicates a rumor through online channels per unit of time, C denotes the average number of times per unit of time that an individual communicates a rumor through offline channels, and C_0 denotes the average number of times per unit of time that an individual communicates a rumor through an online channel that causes ego depletion.

Second, there is a competitive relationship between the mass media layer M and the online social network layer A. Mass media will inhibit the spread of rumors in the online social network layer by releasing rumor-debunking information through new media, such as public numbers and today's headlines, etc., and, in turn, the frequency of an individual's use of online nonmainstream news sources will affect the degree to which the mass media's information is effective in influencing him or her [40,41], i.e., the greater the number k of times an individual is exposed to rumors in the online social network layer A, the greater the degree to which mass media's messages are effective in influencing them. This effect will be reflected in the weakening of the mass media's inhibition of rumor propagation rates in the online network layer A. That is

$$\Theta^{A\to M} = \theta\left(1 - e^{-\frac{\alpha_1}{k}}\right), \tag{19}$$

$$\Theta^{M\to A} = 1 - \frac{u_1 m_1 \Theta^{A\to M}\Theta^{B\to M}}{\alpha + u_1 m_1 \Theta^{A\to M}\Theta^{B\to M}}, \tag{20}$$

where α_1 denotes an individual's level of trust in the new mass media, u_1 denotes the influence strength of new mass media on the online propagation channel, α is the half-saturation constant.

Finally, there is also a competitive relationship between the mass media layer M and the offline physical contact layer B. The mass media also releases rumor-debunking information through traditional media, such as TV and newspapers, to inhibit the spread of rumors in the offline contact network layer. Similarly, the frequency of individuals' use of the offline contact network layer B also affects the effectiveness of mass media messages [40,41], i.e., the greater the number of times C that individuals are exposed to rumors in the offline physical contact network layer B, the greater the impact of mass media messages on them. This effect is also reflected in the weakening of the mass media's inhibition of rumor propagation rates

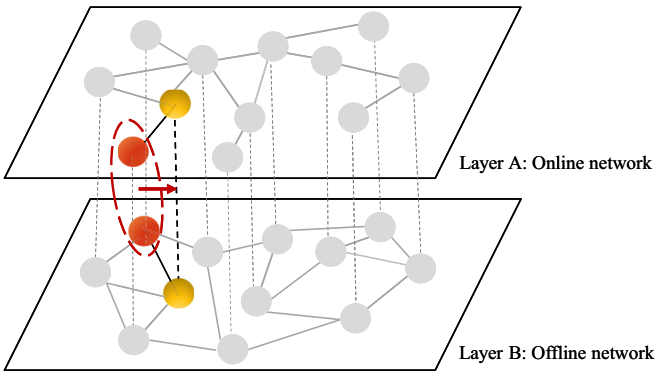


FIG. 3. Illustration of the positive social reinforcement effect. Ignorant individuals (I) exposed to identical rumor stimuli from both online and offline neighbors are more likely to adopt and spread the rumor, reflecting increased persuasion under multiple social influences.

in the offline physical contact layer B. That is

$$\Theta^{B\to M} = \theta\left(1 - e^{-\frac{\alpha_2}{C}}\right), \tag{21}$$

$$\Theta^{M\to B} = 1 - \frac{u_2 m_2 \Theta^{A\to M}\Theta^{B\to M}}{\alpha + u_2 m_2 \Theta^{A\to M}\Theta^{B\to M}}, \tag{22}$$

where α_2 denotes an individual's level of trust in the traditional mass media, u_2 denotes the influence strength of traditional mass media on the offline propagation channel.

4. Social reinforcement rules

Individuals' behaviors are not only influenced by their neighbors in the online network, but also by their neighbors in the offline network, so we should also consider the influence of the social reinforcement effect, which is different from the previous studies, this paper considers the different responses of individuals in different states to the social reinforcement effect. That is, when individuals who do not know the rumor are receiving the same information stimulus from different social circles, they are more likely to be persuaded and have a higher possibility of propagating the rumor, and we call this process the positive social reinforcement effect, as shown in Fig. 3. This study assumes that when a single-channel spreader receives the same information stimulus from a different social circle, he will lose his interest in spreading because he already knows the information and will think that this information is already known to most people, and we call this process the negative social reinforcement effect, as shown in Figs. 4(a) and 4(b).

Therefore, we define the following social reinforcement intensity:

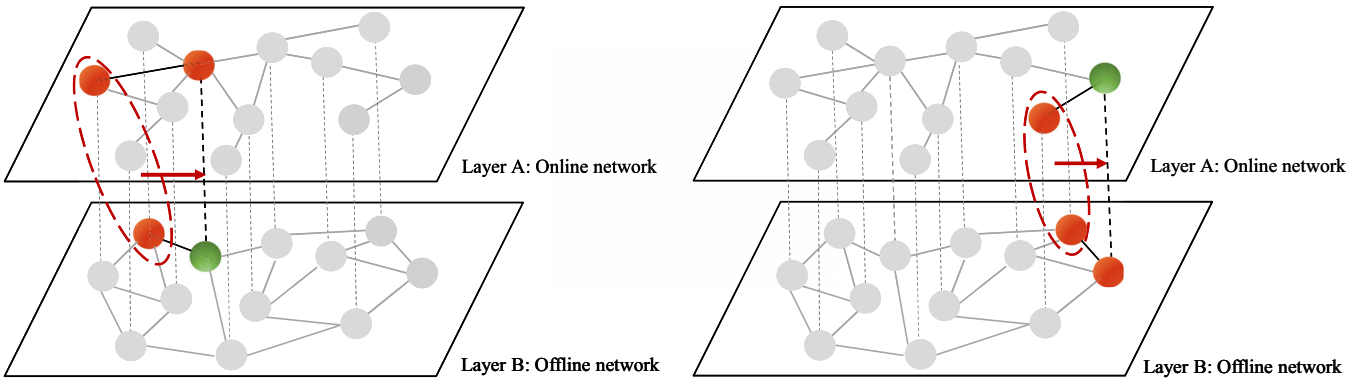
$$\delta(t) = \delta_0 \Theta^{M\to A}[1 - (1 - i(t) - s_1(t) - r(t))^{\langle k\rangle}]\Theta^{M\to B} \times [1 - (1 - i(t) - s_2(t) - r(t))^{C}], \tag{23}$$

where $(1 - (1 - i(t) - s_1(t) - r(t))^{\langle k\rangle})$ is the probability that an individual in the online network layer has at least one spreader neighbor, $(1 - (1 - (i(t) - s_2(t) - r(t))^{C})$ is the probability that an individual in the offline network layer has at least one spreader neighbor. δ_0 is the probability that an individual switches states under the influence of social reinforcement. $\Theta^{M\to A}$ is the inhibitory effect of mass media on the intensity of social reinforcement in the online communication channel, and $\Theta^{M\to B}$ is the inhibitory effect of mass media on the intensity of social reinforcement in the online propagation channel.

Specifically, a positive social reinforcement effect means that an ignorant person converts to a dual-channel spreader with a probability of $\delta(t)$ when both channels each have at least one spreader neighbor; a negative social reinforcement effect means that a single-channel spreader loses interest in propagating and converts to a stifler with a probability of $\delta(t)$ when both channels each have at least one spreader neighbor. Dual-channel spreaders are assumed to be immune to social reinforcement because of their stronger willingness to spread.

C. Mean-field analysis

Based on the propagation rules introduced above, we derive the mean-field equations governing the temporal evolution of the five population states (I, S_1, S_2, S_3, R). To



(a) (b)

FIG. 4. Illustration of the negative social reinforcement effect. (a) An online single-channel spreader $S_1(S_A R_B)$ receiving identical rumor stimuli from offline neighbors loses interest in further spreading, considering the information already widely known. (b) An offline single-channel spreader $S_2(R_A S_B)$ receiving identical rumor stimuli from online neighbors undergoes the same reduction in spreading activity.

simplify the notation, we introduce the auxiliary quantities $\phi_Z^A = \sum_{l=0}^{n} p(l/k)\frac{Z_{(m_1,m_2,l,C)}}{N_{(m_1,m_2,l,C)}}$ and $\phi_Z^B = \frac{1}{N}\sum_{l=0}^{n} Z_{(m_1,m_2,l,C)}$, representing the probabilities of contacting a Z-type individual through online and offline communication, respectively, where $Z \in \{I, S_1, S_2, S_3, R\}$. Each equation follows directly from the corresponding state transition rules described in the previous subsection. The resulting mean-field system is given by

$$
\begin{aligned}
\frac{dI_{(m_1,m_2,k,C)}(t)}{dt} &= \Lambda N - \Theta^{M\to A}\omega\beta_A\Theta^{B\to A}kI_{(m_1,m_2,k,C)}\phi_{S_1}^A - \Theta^{M\to A}\beta_A k\Theta^{B\to A}I_{(m_1,m_2,k,C)}\phi_{S_3}^A - (\mu+\delta(t))I_{(m_1,m_2,k,C)} \\
&\quad - \Theta^{M\to B}\beta_B\Theta^{A\to B}CI_{(m_1,m_2,k,C)}\phi_{S_3}^B - \Theta^{M\to B}\omega\beta_B\Theta^{A\to B}CI_{(m_1,m_2,k,C)}\phi_{S_2}^B + \eta R_{(m_1,m_2,k,C)} \\
\frac{dS_{1(m_1,m_2,k,C)}(t)}{dt} &= \Theta^{M\to A}\omega\beta_A\Theta^{B\to A}kI_{(m_1,m_2,k,C)}\phi_{S_1}^A - \omega\alpha_A kS_{1(m_1,m_2,k,C)}\phi_{S_2}^A + \Theta^{M\to A}\beta_A\Theta^{B\to A}kI_{(m_1,m_2,k,C)}\phi_{S_3}^A \\
&\quad - \alpha_A kS_{1(m_1,m_2,k,C)}\phi_{S_3}^A - \Theta^{M\to B}\omega\beta_B\Theta^{A\to B}CS_{1(m_1,m_2,k,C)}\phi_{S_2}^B - \Theta^{M\to B}\beta_B\Theta^{A\to B}CS_{1(m_1,m_2,k,C)}\phi_{S_3}^B \\
&\quad + \omega\alpha_B CS_{3(m_1,m_2,k,C)}\phi_{S_1}^B + \alpha_B CS_{3(m_1,m_2,k,C)}\phi_R^B - (\mu+\delta(t))S_{1(m_1,m_2,k,C)} \\
\frac{dS_{2(m_1,m_2,k,C)}(t)}{dt} &= -\Theta^{M\to B}\omega\beta_B\Theta^{A\to B}kS_{2(m_1,m_2,k,C)}\phi_{S_1}^A + \omega\alpha_A kS_{3(m_1,m_2,k,C)}\phi_{S_2}^A - \Theta^{M\to B}\beta_B\Theta^{A\to B}kS_{2(m_1,m_2,k,C)}\phi_{S_3}^A \\
&\quad + \alpha_A kS_{3(m_1,m_2,k,C)}\phi_R^A + \Theta^{M\to B}\omega\beta_B\Theta^{A\to B}CI_{(m_1,m_2,k,C)}\phi_{S_2}^B + \Theta^{M\to B}\beta_B\Theta^{A\to B}CI_{(m_1,m_2,k,C)}\phi_{S_3}^B \\
&\quad - \omega\alpha_B CS_{2(m_1,m_2,k,C)}\phi_{S_1}^B - \alpha_B CS_{2(m_1,m_2,k,C)}\phi_R^B - (\mu+\delta(t))S_{2(m_1,m_2,k,C)} \\
\frac{dS_{3(m_1,m_2,k,C)}(t)}{dt} &= \Theta^{M\to B}\omega\beta_B\Theta^{A\to B}kS_{2(m_1,m_2,k,C)}\phi_{S_1}^A - \omega\alpha_A kS_{3(m_1,m_2,k,C)}\phi_{S_2}^A + \Theta^{M\to B}\beta_B\Theta^{A\to B}kS_{2(m_1,m_2,k,C)}\phi_{S_3}^A \\
&\quad - \alpha_A kS_{3(m_1,m_2,k,C)}\phi_R^A + \Theta^{M\to B}\omega\beta_B\Theta^{A\to B}CS_{1(m_1,m_2,k,C)}\phi_{S_2}^B + \Theta^{M\to B}\beta_B\Theta^{A\to B}CS_{1(m_1,m_2,k,C)}\phi_{S_3}^B \\
&\quad - \omega\alpha_B CS_{3(m_1,m_2,k,C)}\phi_{S_1}^B - \alpha_B CS_{3(m_1,m_2,k,C)}\phi_R^B - \mu S_{3(m_1,m_2,k,C)} + \delta(t)I_{(m_1,m_2,k,C)} \\
\frac{dR_{(m_1,m_2,k,C)}(t)}{dt} &= \omega\alpha_A kS_{1(m_1,m_2,k,C)}\phi_{S_2}^A + \alpha_A kS_{1(m_1,m_2,k,C)}\phi_R^A + \omega\alpha_B CS_{2(m_1,m_2,k,C)}\phi_{S_1}^B + \alpha_B CS_{2(m_1,m_2,k,C)}\phi_R^B \\
&\quad - (\mu+\eta)R_{(m_1,m_2,k,C)} + \delta(t)S_{1(m_1,m_2k,C)} + \delta(t)S_{2(m_1,m_2,k,C)}.
\end{aligned}
\tag{24}
$$

The first equation describes the evolution of ignorants, while the remaining equations correspond to online single-channel spreaders, offline single-channel spreaders, dual-channel spreaders, and stiflers, respectively. Each term represents one of the spreading, transition, recovery, or demographic processes defined in the previous subsection. The meanings of the system-related parameters are provided in Table S1 of the Supplemental Material (SM) [42].

III. RESULTS

To derive the threshold condition for rumor propagation in the multilayer coupled network, we assume that the network is degree-uncorrelated, i.e., $p(l|k) = \frac{lp(l)}{<k>} = \frac{lN(l)}{<k>N}$. Following the standard next-generation matrix approach [43,44], we decompose the linearized system around the rumor-free equilibrium into the new infection matrix F and the transition matrix V. The basic reproduction number is then given by $R_0 = \rho(FV^{-1})$, where $\rho(\cdot)$ denotes the spectral radius of the next-generation matrix. Owing to the high dimensionality of the proposed model, the explicit expressions of F, V, and the derivation of Eq. (25) are provided in Appendix A of SM [42]:

$$
\begin{aligned}
R_0 = \frac{1}{2\mu(\mu+\delta_0)^2}\Bigg[&\Theta^{M\to A}\Theta^{B\to A}(\mu\omega\beta_A+\beta_A)\frac{\langle k^2\rangle}{\langle k\rangle} \\
&+ \Theta^{M\to B}\Theta^{A\to B}(\mu\omega\beta_B+\theta\beta_B)C + \sqrt{\Delta}\Bigg],
\end{aligned}
\tag{25}
$$

where $\Delta = (\Theta_1(\mu\omega\beta_A+\beta_A)\frac{\langle k^2\rangle}{\langle k\rangle} - \Theta_2(\mu\omega\beta_B+\theta\beta_B)C)^2 + 4\Theta_1(\mu\omega\beta_A+\beta_A)\Theta_2(\mu\omega\beta_B+\theta\beta_B)C\langle k\rangle$, $\Theta_1 = \Theta^{M\to A}\Theta^{B\to A}$, $\Theta_2 = \Theta^{M\to B}\Theta^{A\to B}$, $\langle k^2\rangle = \sum_{k=0}^{n} k^2 p(k)$, $\Theta^{M\to A} = 1-\frac{u_1 m_1\Theta^{A\to M}\Theta^{B\to M}}{\alpha+u_1 m_1\Theta^{A\to M}\Theta^{B\to M}}$, $\Theta^{B\to A} = \frac{\theta C}{C+|C_0-C|}$, $\Theta^{M\to B} = 1-\frac{u_2 m_2\Theta^{A\to M}\Theta^{B\to M}}{\alpha+u_2 m_2\Theta^{A\to M}\Theta^{B\to M}}$, $\Theta^{A\to B} = \frac{\theta<k>}{<k>+|C_0-<k>|}$, $\Theta^{A\to M} = \theta(1-e^{-\frac{\alpha_1}{k}})$, $\Theta^{B\to M} = \theta(1-e^{-\frac{\alpha_2}{C}})$.

We next investigate the rumor propagation dynamics under cooperative and competitive interactions among the three communication channels through numerical simulations. Unless otherwise specified, all numerical simulations were performed using MATLAB R2019b (MathWorks, Natick, MA, USA). We use the hour as the unit time. The online network is assumed to be a scale-free network whose degree distribution satisfies $p(k) = (\varpi-1)\vartheta^{\varpi-1}k^{-\varpi}$ and the parameters are chosen as $\varpi = \vartheta = 3$. The offline network is a homogeneous mixed network.

The parameter settings can be divided into two categories. The baseline parameter values are selected with reference to commonly adopted settings in previous rumor propagation studies [13,15,18,22]. Specifically, we set $\Lambda = 0.2$, $\beta_A = 0.4$, $\beta_B = 0.2$, $\mu = 0.17$, $\delta_0 = 0.5$, and $\theta = 0.9$. The remaining parameters do not have reliable empirical estimates in the existing literature and are therefore chosen within plausible ranges to explore the effects of different spreading mechanisms.

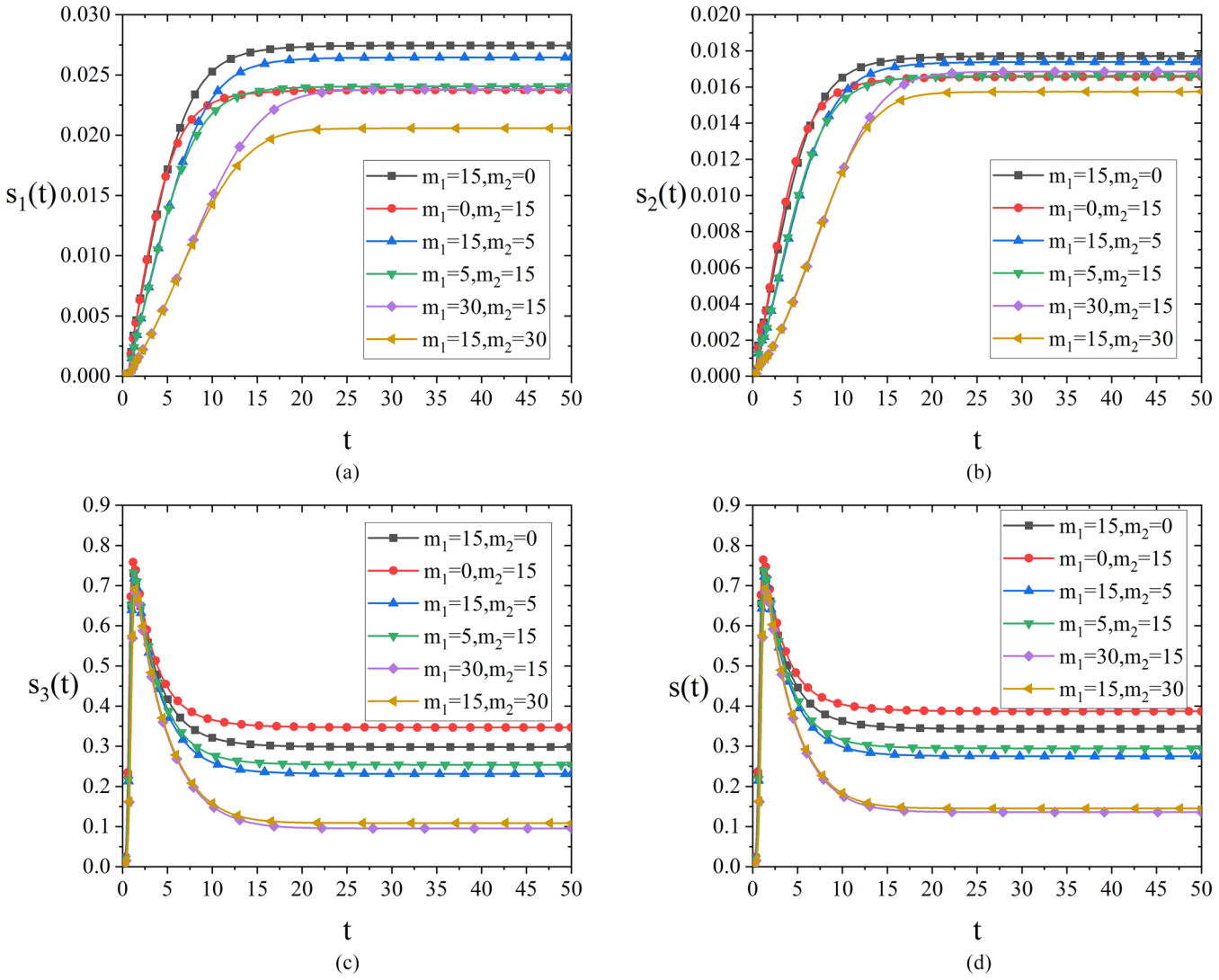


FIG. 5. Time evolution of (a) online single-channel spreader density s_1, (b) offline single-channel spreader density s_2, (c) dual-channel spreader density s_3, and (d) total spreader density s under six mass media intervention scenarios, defined by different combinations of emerging mass media intensity m_1 and traditional mass media intensity m_2. Black and red lines correspond to new-media-only ($m_1 = 15, m_2 = 0$) and traditional-media-only ($m_1 = 0, m_2 = 15$) interventions, respectively; blue and green lines represent moderate combined interventions ($m_1 = 15, m_2 = 5$) and ($m_1 = 5, m_2 = 15$); purple and yellow lines denote stronger combined interventions ($m_1 = 30, m_2 = 15$) and ($m_1 = 15, m_2 = 30$). Panel (a) shows that increasing m_2 slows both the growth rate and eventual level of s_1, while increasing m_1 under fixed m_2 slows the rate but has little impact on the final value. In contrast, panel (b) reveals that s_2 is consistently better suppressed by traditional media, especially in final value. Panel (c) indicates that s_3 shows the opposite trend, where new media interventions are more effective. Panel (d) exhibits similar dynamics to panel (c), though the overall density is higher due to the additive contributions of s_1 and s_2. These results support a hybrid intervention strategy: allocate traditional media to control offline and online single-channel spreaders, while using new media to curb dual-channel transmission.

A. Effects of mass media intervention

The first set of simulations focuses on the influence of mass media interventions. To examine how different mass media interventions influence rumor dynamics across multiple spreader types, Fig. 5 presents the temporal evolution of four key variables: online single-channel spreaders (s_1), offline single-channel spreaders (s_2), dual-channel spreaders (s_3), and the total spreader density (s). Six intervention scenarios are simulated, varying the intensity of new media (m_1) and traditional media (m_2) interventions.

In Fig. 5(a), s_1 is more effectively suppressed by stronger traditional media intervention. When comparing the red ($m_1 = 0, m_2 = 15$) and black ($m_1 = 15, m_2 = 0$) lines, the red stabilizes at a lower level, suggesting that offline interventions can indirectly constrain online spreaders. Additionally, when m_1 is fixed (black, blue, yellow), increasing m_2 gradually reduces both the growth rate and peak value of s_1. However, when m_2 is fixed (red, green, purple), increasing m_1 slows the growth rate but has minimal effect on the final spreader level.

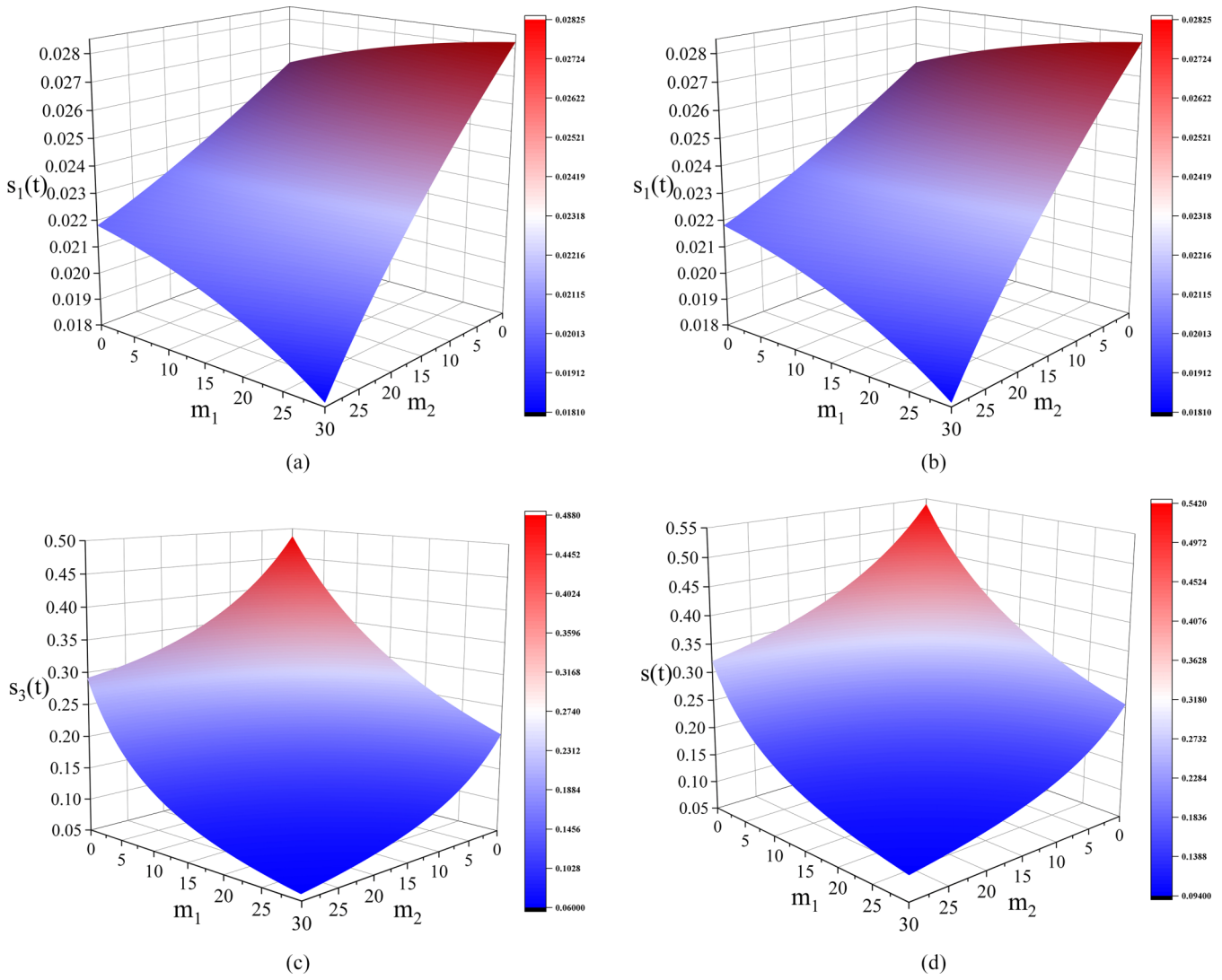


FIG. 6. Evolution of the densities of (a) online single-channel spreaders s_1, (b) offline single-channel spreaders s_2, (c) dual-channel spreaders s_3, and (d) total spreaders $s = s_1 + s_2 + s_3$ as functions of the intervention intensities of new mass media m_1 and traditional mass media m_2. Overall, increasing both m_1 and m_2 suppresses the spreader densities, yet complex nonlinear interactions emerge. Interestingly, for small m_2, increasing m_1 leads to a rise in s_1, reflecting a compensatory effect where insufficient offline intervention allows spillover into the online domain. For s_2, a reversal from decline to growth emerges under strong m_2 and rising m_1, driven by a redistribution of dual-channel spreaders into the offline layer and a breakdown of cross-layer suppression. s_3 decreases monotonically, with m_1 exerting a stronger suppressive effect than m_2. The total spreader density s exhibits a composite pattern, with new mass media interventions being more effective overall, though the relative differences narrow compared to s_3, due to the contribution of single-channel spreaders.

In Fig. 5(b), s_2 shows higher sensitivity to traditional media interventions. For example, while the black and red lines rise at similar rates, the red stabilizes at a significantly lower value, indicating better control under traditional media. This pattern persists across all scenarios—stronger m_2 consistently reduces the steady-state s_2, while increased m_1 mainly delays its rise.

Figure 5(c) reveals a reversed pattern for dual-channel spreaders: s_3 is more sensitive to new media interventions. In all comparisons (e.g., red vs black, green vs blue), the scenarios with stronger m_1 yield lower final densities. This indicates that dual-channel spreaders are more tightly coupled to online propagation dynamics and are more susceptible to regulation within online media environments.

Figure 5(d) integrates the trends from all spreader types. While its shape mirrors s_3, the absolute values are higher due to cumulative contributions from s_1 and s_2.

These results highlight the need for differentiated strategies: traditional media is better suited for controlling single-channel spreaders, whereas new media is more effective in suppressing dual-channel spreaders. Strategic allocation of intervention resources can synergistically reduce overall rumor propagation.

Figure 6(a) illustrates the dependence of the online single-channel spreader density s_1 on the intervention intensities m_1 and m_2. Although increasing both interventions generally suppresses s_1, a notable exception occurs when traditional media intervention m_2 is weak: increasing new

media intervention m_1 paradoxically amplifies s_1. This counterintuitive behavior arises from a compensatory feedback mechanism—insufficient offline suppression allows ongoing offline transmission and sustains dual-channel spreaders s_3, which, when pressured by elevated m_1, migrate into the online single-channel class s_1. Furthermore, the lack of coordinated dual-layer control weakens cross-layer suppression, enabling offline-originated spreading influence to flow back into the online domain. This interplay highlights the necessity of synchronized interventions across media channels to prevent unintended amplification effects.

Figure 6(b) shows the variation of offline single-channel spreader density s_2 under varying new mass media intervention intensity m_1 and traditional mass media intervention intensity m_2. As expected, s_2 declines with stronger traditional media intervention. However, the suppressive effect of m_2 is significantly modulated by m_1: a given increase in m_2 yields a sharper reduction in s_2 when m_1 is low. Intriguingly, under strong m_2, increasing m_1 reverses the expected trend, leading to an increase in s_2, which we attribute to a nonlinear redistribution of dual-channel spreaders s_3 into the offline layer, driven by intensified cross-layer pressure and a breakdown in coordinated suppression.

Figure 6(c) presents the response of the dual-channel spreader density s_3 to increasing m_1 and m_2. The suppression is monotonic in both dimensions, yet the gradient is steeper along m_1, suggesting that new mass media interventions exert a more potent influence on dual-layer dynamics. This indicates asymmetry in channel dominance and intervention efficacy, with new media being structurally more disruptive to dual-channel spreaders.

Figure 6(d) tracks the total spreader density $s = s_1 + s_2 + s_3$ as a function of m_1 and m_2. The trend broadly mirrors that of s_3, though overall magnitudes are elevated due to contributions from single-channel spreaders. The efficacy of m_1 in reducing s remains higher than m_2, albeit the difference is less pronounced compared to s_3, indicating a more distributed sensitivity across channels. This underscores the importance of synchronized multi-channel interventions to achieve systemic containment.

B. Effect of heterogeneous initial channel preferences

Next, to examine the impact of initial channel-specific spreader composition on rumor propagation dynamics, Fig. 7 presents the temporal evolution of the total spreader density $s(t)$ under three distinct initial conditions: a dominant initial proportion of online single-channel spreaders (s_1, black line), dual-channel spreaders (s_3, red line), and offline single-channel spreaders (s_2, blue line), respectively. The results reveal clear differences in propagation velocity and intensity across these scenarios.

The system exhibits the most rapid and extensive spread when dual-channel spreaders s_3 dominate the initial state, as evidenced by the steep rise of the red curve. This is attributed to their ability to simultaneously access both online and offline pathways, maximizing reach and cross-layer influence. In contrast, when online single-channel spreaders s_1 are initially predominant, the propagation remains relatively fast (black line), driven by the high efficiency and low latency

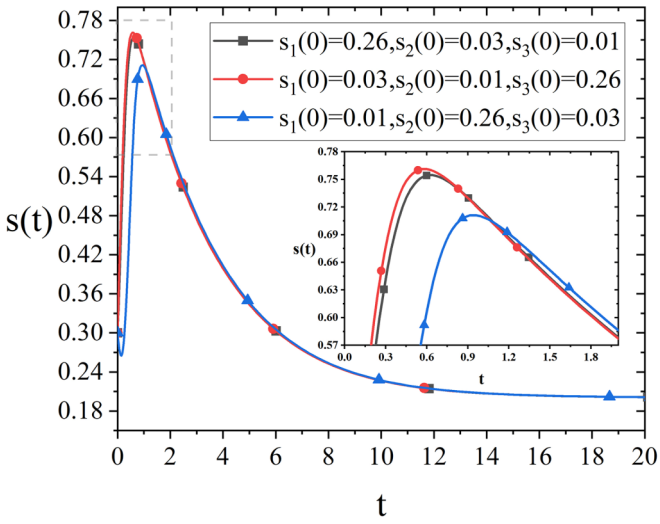


FIG. 7. Time evolution of the total spreader density $s(t)$ under three distinct initial conditions: dominant presence of online single-channel spreaders (s_1, black line), dual-channel spreaders (s_3, red line), and offline single-channel spreaders (s_2, blue line). The propagation is fastest and most intense when s_3 is initially dominant, followed by s_1, while the slowest and weakest spread occurs when s_2 dominates. These dynamics reflect the varying propagation capacities of different channel types, with dual-channel spreaders exerting the strongest influence due to their simultaneous access to both online and offline networks.

of online communication, though its impact is limited by the single-layer constraint. The slowest growth occurs when offline single-channel spreaders s_2 dominate (blue line), reflecting the lower transmission efficiency and spatial-temporal constraints inherent in offline dissemination.

These results highlight the system's sensitivity to initial channel composition and demonstrate that dual-channel spreaders possess the highest propagation capacity due to their cross-channel accessibility. Online spreaders follow with moderate impact, while offline spreaders exert the weakest influence due to structural and temporal limitations.

C. Cooperation-to-competition transition between online and offline channels

Furthermore, the two primary rumor propagation channels—online and offline—interact in complex ways that substantially influence the overall dynamics. To explore this interplay, Fig. 8 examines how the cooperative and competitive interactions between these channels affect the steady-state densities of different spreader types. Here, the x-axis denotes the average online propagation frequency per unit time, $\langle k \rangle$, capturing either the activity level of spreaders or the rumor's popularity within online networks. The y-axis represents the corresponding offline propagation frequency, C, serving as an analog for offline engagement intensity or offline rumor salience.

To quantitatively characterize the interactions between online and offline channels, the steady-state data obtained from numerical simulations were fitted using Response Surface Methodology (RSM) in Design-Expert. The resulting fitted

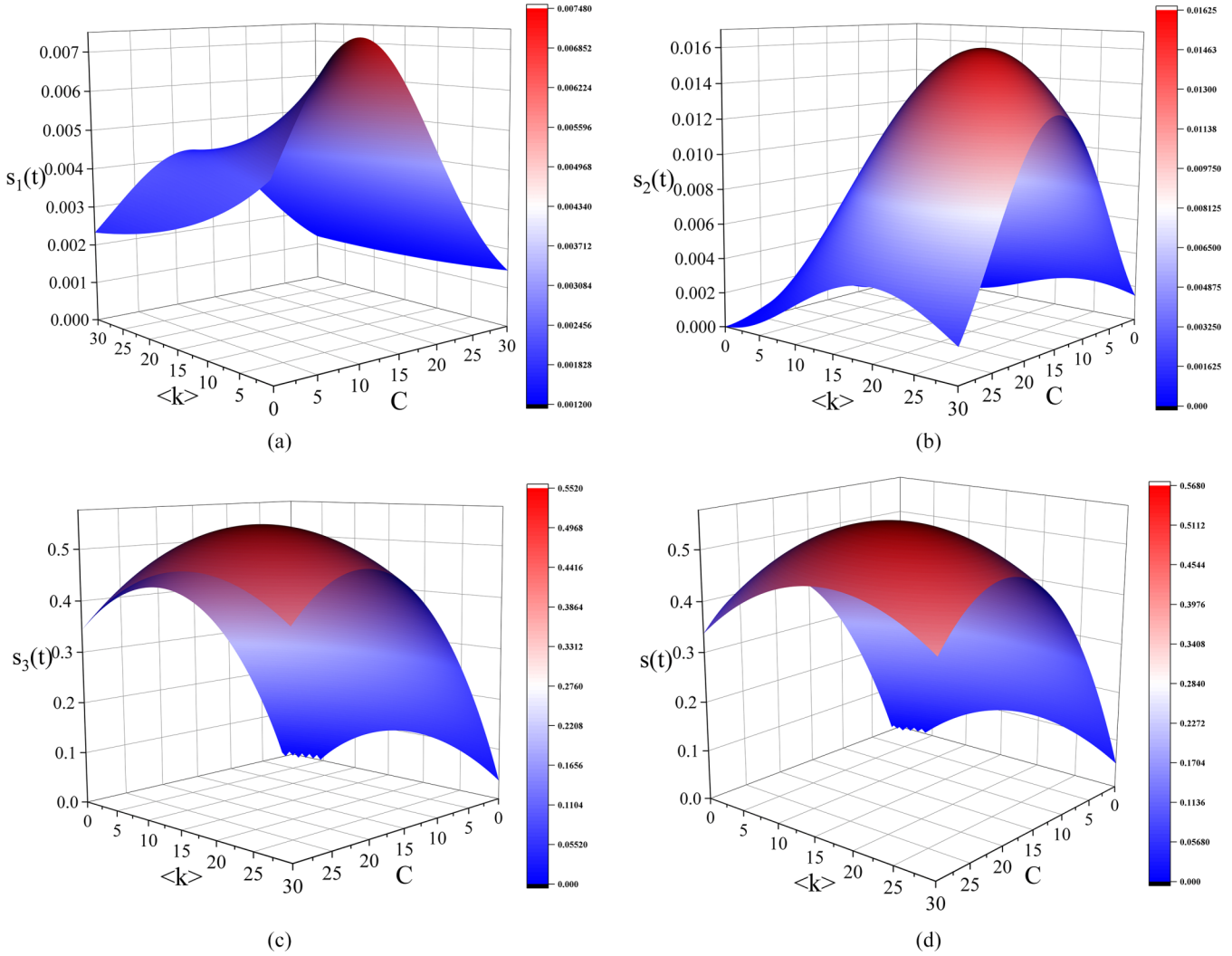


FIG. 8. Effects of average rumor propagation frequency in online ($\langle k \rangle$) and offline (C) channels on the densities of (a) online single-channel spreaders s_1, (b) offline single-channel spreaders s_2, (c) dual-channel spreaders s_3, and (d) total spreaders s. In panel (a), increasing C first enhances and then suppresses s_1, revealing a cooperation-to-competition shift between channels; s_1 also decreases monotonically with $\langle k \rangle$, reflecting increased conversion to s_3. In (b), s_2 exhibits a nonmonotonic response to both parameters, with a response-surface peak located at $\langle k \rangle = 22.06, C = 16.11$, marking a saturation threshold where inter-channel dynamics transition from mutual reinforcement to competition. In (c), s_3 follows a similar trend, peaking at $\langle k \rangle = 17.46, C = 21.22$, suggesting greater sensitivity to online activity. The overall spreader density s in (d) mirrors the behavior of s_3, confirming the dominant role of dual-channel spreaders in driving system-wide rumor propagation.

empirical equations were subsequently used to construct the response surfaces shown in Fig. 8. These empirical response surfaces provide a quantitative description of the parameter regions in which increasing $\langle k \rangle$ or C changes from promoting rumor propagation to suppressing it. A quantitative characterization of these transitions based on the RSM results is provided in Appendix B of SM [42].

Figure 8(a) offline rumor propagation frequency C and online propagation frequency $\langle k \rangle$ on the density of online single-channel spreaders s_1. When $\langle k \rangle$ is fixed, increasing C initially promotes s_1, but beyond a critical threshold (around $C = 10$), further increases in C lead to its decline. This nonmonotonic response indicates a shift from cooperation to competition between the two channels: moderate offline popularity reinforces online diffusion, but excessive offline propagation suppresses the role of online-only spreaders, likely due to competition for influence or the conversion of spreaders. Additionally, s_1 decreases consistently with increasing $\langle k \rangle$, suggesting that higher online rumor popularity encourages online spreaders to transition into dual-channel behavior (s_3). Sensitivity analysis also shows that when $\langle k \rangle$ is low, s_1 is more responsive to changes in C, whereas this sensitivity diminishes as $\langle k \rangle$ grows—implying a dynamic shift in channel dominance based on rumor intensity.

Figure 8(b) shows that the offline single-channel spreader density s_2 responds nonmonotonically to increases in both $\langle k \rangle$ and C. Within a moderate range, rising rumor popularity in either channel reinforces overall spread, increasing s_2. However, beyond $\langle k \rangle = 22.06$ and $C = 16.11$, the system reaches a saturation point, and further increases lead to a decline in s_2. This turning point marks the transition from cooperative enhancement to inter-channel competition, indicating that excessive

multi-channel rumor heat may cause offline-only spreaders to be either suppressed or absorbed into other categories (e.g., s_3).

In Fig. 8(c), the dual-channel spreader density s_3 exhibits a trend similar to s_2, with an initial increase followed by a decline as both $\langle k \rangle$ and C grow. This again reflects a cooperation-to-competition transition, but with a distinct sensitivity profile: the peak in s_3 occurs at $\langle k \rangle = 17.46$, $C = 21.22$, earlier than in s_2, indicating that dual-channel spreaders are more sensitive to changes in online propagation intensity. This aligns with their ability to operate in both channels, making them more responsive to shifts in online activity levels.

Figure 8(d) presents the total spreader density s under varying $\langle k \rangle$ and C. The system-wide dynamics mirror those of the dual-channel population s_3, further confirming their central role in driving the overall spread. The total spreader density increases with rising rumor popularity across both channels up to a critical point, after which saturation and inter-channel competition suppress further spread. This underscores the dominant influence of dual-channel spreaders and the nonlinear character of cross-channel propagation dynamics.

These findings emphasize the importance of considering channel interactions, thresholds, and the nonlinear nature of rumor dynamics when designing control strategies. Effective rumor mitigation requires balancing interventions across both online and offline domains, taking into account how different levels of channel activity can shift the system from reinforcement to competition.

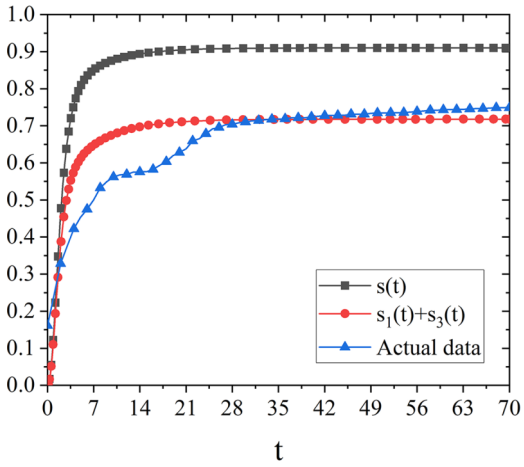


FIG. 9. Model validation through empirical fitting with real-world Twitter data. The blue line represents the time evolution of online rumor spreaders extracted from a cleaned dataset containing 1116 tweets and retweets labeled as rumors during the Kavanaugh hearing. The red line shows the corresponding model output for the density of online spreaders, defined as the sum of online single-channel spreaders and dual-channel spreaders. The gray line represents the total spreader density in the model. The close alignment between the red and blue curves confirms that the model accurately captures the real-world dynamics of online rumor propagation. The deviation between the gray and blue lines highlights the presence of offline single-channel spreaders not observable in the Twitter dataset, indicating that the full model can infer hidden offline dynamics and guide differentiated interventions.

D. Model validation using Twitter data

To assess the validity and practical applicability of the proposed model, we further perform empirical verification using real-world data. Specifically, we fit the system to a dataset obtained from Twitter [45], which records the data entitled "During confirmation hearings for Supreme Court nominee Brett Kavanaugh, congressional Democrats demanded that the nominee undergo DNA testing to prove he is not Adolf Hitler". The dataset includes original tweets and retweets, labeled by tweet status, user ID, timestamp, and other metadata. Tweets marked with an "r" status are identified as rumor-related and are used to define the propagator population in the model.

After preprocessing to remove incomplete entries, a total of 1,116 valid records were retained. Detailed information about the dataset, preprocessing steps, and sample entries is provided in SM (Table S2) [42]. Model fitting was conducted using only the online spreader component (the sum of online single-channel spreaders s_1 and dual-channel spreaders s_3), as the data reflect online propagation. Parameter values used in the fitting are listed in SM Table S3 [42], and the fitting results are illustrated in Fig. 9.

In Fig. 9, the gray line represents the time evolution of the density of all spreaders in the model, the red line represents the time evolution of the density of online spreaders (including online single-channel spreaders s_1 and dual-channel spreaders s_3) in the model, and the blue line represents the actual Twitter dataset. It can be observed that the red line fits better with the blue line, indicating that the time evolution of online spreaders in the model more accurately simulates the real data and verifies the model's validity.

In addition, the large difference between the gray line and the blue line indicates that there is a significant difference between the total spreader density s and the trend of the real data, and this difference is mainly due to the existence of offline single-channel spreaders. Therefore, the relevant management departments can use the model in this paper to predict the spread of offline rumors and take targeted measures for different types of spreaders to more accurately understand and predict the spreading dynamics of rumors.

IV. DISCUSSION AND CONCLUSIONS

This study investigated how heterogeneous communication behaviors, heterogeneous mass media, and social reinforcement jointly reshape rumor propagation dynamics across multiple communication channels. To address this question, we developed a multilayer rumor propagation framework integrating these mechanisms and analyzed its dynamical behavior using mean-field theory. The propagation threshold was derived through the next-generation matrix method, and the theoretical results were further supported by numerical simulations and validated using Twitter data. This unified framework enables the interplay among these mechanisms to be analyzed systematically within a common dynamical system.

The findings highlight the differential influence of mass media interventions across spreader types. Traditional media interventions proved most effective in curbing single-channel spreaders, particularly those active in offline settings. In contrast, new mass media interventions had a stronger impact on dual-channel spreaders, who operate simultaneously in online and offline networks. These results suggest that the design of intervention strategies should consider not only the type of rumor and its audience but also the specific characteristics of spreaders. Policies that overlook this heterogeneity may underestimate the influence of certain groups or misallocate resources.

The results also reveal important interactions between traditional and new media. When traditional media pressure is relatively weak, new media interventions can reduce the prevalence of offline spreaders to some degree. However, once traditional media interventions become strong, additional efforts by new media may yield diminishing or even counterproductive effects. Such outcomes could increase control costs or, in some cases, amplify unintended side effects. This observation underscores the need for careful calibration of interventions, as uncoordinated media campaigns may undermine their own effectiveness.

Another central insight concerns the dynamics between online and offline channels. At the early stage of propagation, these channels tend to reinforce one another, as exposure in one space enhances the likelihood of activity in the other. Over time, however, competition emerges. Individuals have limited cognitive and temporal resources, and as one channel dominates attention, engagement in the other may decline. This shift indicates that the interaction between online and offline communication channels is dynamic rather than static, providing a mechanistic explanation for the evolution of rumor propagation in heterogeneous communication systems. Dual-channel spreaders are especially sensitive to changes in online rumor prevalence, suggesting that online activity often serves as a leading indicator for broader propagation trends.

Our analysis further demonstrates the critical role of dual-channel spreaders. Unlike single-channel spreaders, who are confined to either online or offline networks, dual-channel spreaders bridge the two environments and exert disproportionate influence on the overall dynamics. Their sensitivity to online fluctuations and their ability to amplify rumors across contexts make them central drivers of rumor cascades. These findings demonstrate that heterogeneous communication behaviors are not merely individual-level characteristics but fundamentally reshape the collective dynamics of rumor propagation across multiple communication channels.

The empirical validation using Twitter data adds practical relevance to the model. By aligning theoretical predictions with real-world dynamics, we show that the model can capture not only online propagation but also its implications for offline spread. This predictive capacity is particularly valuable for policymakers and authorities, as it provides a tool for anticipating offline consequences of online activity and for designing interventions that address spreaders across different channels. Such applications highlight the model's potential to inform practical strategies for rumor management.

Despite these contributions, several avenues remain for future research. First, the current model assumes static network structures, yet in reality, social networks are dynamic, with ties forming and dissolving over time. Incorporating adaptive network structures would allow for the simulation of evolving social relationships and their influence on rumor dynamics. Second, while this study focused on behavioral and structural heterogeneity, emotional and psychological factors also play a significant role in rumor acceptance and dissemination. Integrating these dimensions would further extend the proposed framework and provide a more comprehensive understanding of rumor propagation dynamics.

Another promising direction is the study of rumor propagation in multilingual and multicultural contexts. Differences in language, cultural norms, and media ecosystems can significantly shape the pathways and velocity of rumor spread. Comparative studies across cultural settings could yield insights into how interventions should be tailored to specific social environments. Furthermore, incorporating machine learning methods for parameter estimation and optimization could improve the model's accuracy and predictive performance. Such approaches would also help authorities design adaptive, data-driven intervention strategies that respond in real time to changes in rumor dynamics.

In conclusion, this work demonstrates that rumor propagation in heterogeneous communication environments cannot be understood as the simple superposition of multiple communication channels. Instead, the interaction among heterogeneous communication behaviors, social reinforcement, and heterogeneous mass media fundamentally reshapes the collective spreading dynamics. In particular, the shift from cooperation to competition and the distinct dynamical roles of dual-channel spreaders provide new mechanistic insights into rumor propagation on multilayer communication networks. These findings demonstrate that the collective spreading dynamics arise from the interaction among heterogeneous communication behaviors, social reinforcement, and heterogeneous mass media, rather than from any individual mechanism alone. Collectively, these results contribute to a deeper understanding of multilayer rumor dynamics while also providing useful guidance for designing targeted intervention strategies.

ACKNOWLEDGMENTS

Y.D. and L.H. acknowledge partial support from the National Natural Science Foundation of China (Grants No. 72574145 and No. 72174121), and the China Scholar Council State Scholarship Fund (Grant No. 202408310270), and the Program for Professor of Special Appointment (Eastern Scholar) at Shanghai Institutions of Higher Learning, and the Project for the National Social Science Foundation of China (Grant No. 24BGL281). M.P. was supported by the Slovenian Research and Innovation Agency (Grant No. P1-0403). S.B. acknowledges support from the project (Grant No. PGR01177) "Systems with higher order interactions and fractional derivatives for applications to AI and high

performance computing" of the Italian Ministry of Foreign Affairs and International Cooperation.

The authors declare that they have no competing interests.

DATA AVAILABILITY

All the computational codes and data that support the plots and other findings of this study are available from the corresponding author upon reasonable request.

[1] Z. Yu, M. Jiang, Y. Zhang, and X. Cong, A rumor spreading model considering the influence of the internet water army in two-layer coupled networks, Nonlinear Dyn. **114**, 349 (2026).

[2] P. Li, F. Hu, F. Li, *et al.*, SEIAR rumor spreading model with antagonistic states in hypernetworks, Appl. Math. Comput. **508**, 129637 (2026).

[3] H. Hou, Y. Wang, Q. Zhai, Z. Zhou, and Y. Jing, Prediction and optimal control of a time-varying SAPDR rumor spreading model via PINNs, Nonlinear Dyn. **114**, 198 (2026).

[4] M. d S. Islam, T. Sarkar, S. H. Khan, A.-H. Mostofa Kamal, S. M. M. Hasan, A. Kabir, D. Yeasmin, M. A. Islam, K. I. Amin Chowdhury, K. S. Anwar, A. A. Chughtai, and H. Seale, COVID-19–related infodemic and its impact on public health: A global social media analysis, Am. J. Trop. Med. Hyg. **103**, 1621 (2020).

[5] D. J. Daley and D. G. Kendall, Stochastic rumours, IMA J. Appl. Math. **1**, 42 (1965).

[6] D. Maki and M. Thomson, *Mathematical Models and Applications* (Prentice Hall, Englewood Cliffs, NJ, 1973).

[7] D. Zanette, Critical behavior of propagation on small-world networks, Phys. Rev. E **64**, 050901 (2001).

[8] D. Zanette, Dynamics of rumor propagation on small-world networks, Phys. Rev. E **65**, 041908 (2002).

[9] S. Ai, S. Hong, X. Zheng, Y. Wang, and X. Liu, CSRT rumor spreading model based on complex network, Int. J. Intell. Syst. **36**, 1903 (2021).

[10] Y. Moreno, M. Nekovee, and A. F. Pacheco, Dynamics of rumor spreading in complex networks, Phys. Rev. E **69**, 066130 (2004).

[11] L. Yang, Z. Li, and A. Giua, Containment of rumor spread in complex social networks, Inf. Sci. **506**, 113 (2020).

[12] L. Zhu, W. Liu, and Z. Zhang, Delay differential equations modeling of rumor propagation in both homogeneous and heterogeneous networks with a forced silence function, Appl. Math. Comput. **370**, 124925 (2020).

[13] K. Du, R. Fan, D. Wang, X. Xie, X. Xu, and J. Lin, Competitive information spreading model in two-layer networks considering dual debunking mechanisms and time lag effects, Phys. A. **665**, 130479 (2025).

[14] Y. Ding and L. Zhu, Turing instability analysis of a rumor propagation model with time delay on non-network and complex networks, Inf. Sci. **667**, 120402 (2024).

[15] Y. Dong, L. 'A. n Huo, X. Xie, and M. Li, Considering individual game behavior and time delay in the multi-channel rumor propagation model, Commun. Theor. Phys. **76**, 075002 (2024).

[16] L.-L. Xia, G.-P. Jiang, B. o Song, and Y. u-R. Song, Rumor spreading model considering hesitating mechanism in complex social networks, Phys. A. **437**, 295 (2015).

[17] F. Yin, X. Xia, X. Zhang, *et al.*, Modelling the dynamic emotional information propagation and guiding the public sentiment in the Chinese Sina-microblog, Appl. Math. Comput. **396**, 125884 (2021).

[18] L. Huo and J. Gu, The influence of individual emotions on the coupled model of unconfirmed information propagation and epidemic spreading in multilayer networks, Phys. A. **609**, 128323 (2023).

[19] H. Hou, Y. Wang, Q. Zhai, and X. Sun, Optimal Control of Stochastic Fractional Rumor Propagation Model in Activity-Driven networks, Appl. Math. Model. **142**, 115968 (2025).

[20] X. Tong, H. Jiang, J. Qiu, X. Luo, and S. Chen, Dynamic analysis of the IFCD rumor propagation model under stochastic disturbance on heterogeneous networks, Chaos Solitons Fractals **173**, 113637 (2023).

[21] M. Ghosh, P. Das, and P. Das, A comparative study of deterministic and stochastic dynamics of rumor propagation model with counter-rumor spreader, Nonlinear Dyn. **111**, 16875 (2023).

[22] W. Pan, W. Yan, Y. Hu, R. He, and L. Wu, Dynamic analysis of a SIDRW rumor propagation model considering the effect of media reports and rumor refuters, Nonlinear Dyn. **111**, 3925 (2023).

[23] S. Zhai, H. Li, S. Zhu, and J. Ma, A multilayer network model of interaction between rumor propagation and media influence, Chaos **34**, 043104 (2024).

[24] H. Guo and X. Yan, Dynamic modeling and simulation of rumor propagation based on the double refutation mechanism, Inf. Sci. **630**, 385 (2023).

[25] L. Huo and Y. Dong, Analyzing the dynamics of a stochastic rumor propagation model incorporating media coverage, Math. Methods Appl. Sci. **43**, 6903 (2020).

[26] Y. Ma, Q. Zhang, and L. Xie, A study on multi-information diffusion model considering dual social reinforcement effect from the perspective of evolutionary game, Appl. Math. Comput. **492**, 129255 (2025).

[27] M. Zheng, L. Lü, and M. Zhao, Spreading in online social networks: The role of social reinforcement, Phys. Rev. E **88**, 012818 (2013).

[28] J. Xie, F. Meng, J. Sun, X. Ma, G. Yan, and Y. Hu, Detecting and modelling real percolation and phase transitions of information on social media, Nat. Hum. Behav. **5**, 1161 (2021).

[29] J. Sun, L. Feng, J. Xie, *et al.*, Revealing the predictability of intrinsic structure in complex networks, Nat. Commun. **11**, 574 (2020).

[30] S. Simonds, Communication theory and the search for effective feedback, J. Hum. Hypertens. **9**, 5 (1995).

[31] S. Strogatz, Exploring complex networks, Nature (London) **410**, 268 (2001).

[32] M. Newman, The structure and function of complex networks, SIAM Rev. **45**, 167 (2003).

[33] C. Granell, S. Gómez, and A. Arenas, Dynamical interplay between awareness and epidemic spreading in multiplex networks, Phys. Rev. Lett. **111**, 128701 (2013).

[34] C. Granell, S. Gómez, and A. Arenas, Competing spreading processes on multiplex networks: Awareness and epidemics, Phys. Rev. E **90**, 012808 (2014).

[35] H. Zhu, Z. Jin, and X. Yan, A dynamics model of coupling transmission for multiple different knowledge in multiplex networks, Phys. A. **629**, 129199 (2023).

[36] H. Zhu, X. Yan, and Z. Jin, Creative idea diffusion model in the multiplex network with consideration of multiple channels, Commun. Nonlinear Sci. **97**, 105734 (2021).

[37] X. Wu, X. Wu, C.-Y. Wang, B. Mao, J.-A. n Lu, J. Lü, Y. i-C. Zhang, and L. Lü, Synchronization in multiplex networks, Phys. Rep. **1060**, 1 (2024).

[38] DataReportal. 2026. DIGITAL 2026:China. DataReportal. URL: https://datareportal.com/reports/digital-2026-china.

[39] H. Zhu, X. Yan, and Z. Jin, Knowledge transmission model in the multiplex networks with consideration of online and offline channels, Commun. Nonlinear Sci. **108**, 106186 (2022).

[40] J. Strömbäck, Y. Tsfati, H. Boomgaarden, *et al.*, News media trust and its impact on media use: Toward a framework for future research, Ann. Int. Commun. Assoc. **44**, 139 (2020).

[41] A. Kalogeropoulos, J. Suiter, L. Udris, *et al.*, News media trust and news consumption: Factors related to trust in news in 35 countries, Int. J. Commun. **13**, 3672 (2019).

[42] See Supplemental Material at http://link.aps.org/supplemental/10.1103/vxkg-41kp for the detailed derivation of the model equations, response surface analysis, and Twitter dataset details.

[43] O. Diekmann, J. A. P. Heesterbeek, and J. A. J. Metz, On the definition and the computation of the basic reproduction ratio R0 in models for infectious diseases in heterogeneous populations, J. Math. Biol. **28**, 365 (1990).

[44] P. Van den Driessche and J. Watmough, Reproduction numbers and sub-threshold endemic equilibria for compartmental models of disease transmission, Math. Biosci. **180**, 29 (2002).

[45] A. Bodaghi, Newly Emerged Rumors in Twitter [Data set], Zenodo, 2019, http://doi.org/10.5281/zenodo.2563864.